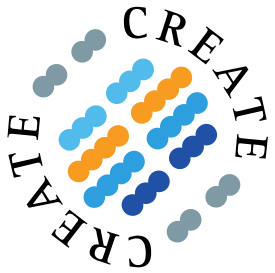

CRITICAL RAW MATERIALS ELIMINATION BY A TOP-DOWN APPROACH TO HYDROGEN AND ELECTRICITY GENERATION

Grant agreement no.: 721065

***Start date**: 01.01.2017 – **Duration**: 42 months*

***Project Coordinator**: CNRS*

DELIVERABLE REPORT

D4.4 – OPTIMIZED AEM & AEI: EX SITU CHARACTERIZATION AND TESTING IN AEMFC AND AEMEL	
Due Date	31/12/2019
Author(s)	Dario Dekel (Technion), Rachel Backhouse (ITM)
Work Package	WP4 - Ionomer synthesis and membrane preparation
Work Package Leader	FUMATECH
Lead Beneficiary	TECHNION
Date released by WP Leader	08/01/2020
Date released by Coordinator	10/01/2020

DISSEMINATION LEVEL		
PU	*Public*	***PU***
PP	*Restricted to other programme participants (including the Commission Services)*	
RE	*Restricted to a group specified by the consortium (including the Commission Services)*	
CO	*Confidential, only for members of the consortium (including the Commission Services)*	

NATURE OF THE DELIVERABLE		
R	*Report*	***R***
P	*Prototype*	
D	*Demonstrator*	
O	*Other*	

SUMMARY	
Keywords	Anion exchange membrane fuel cell, membrane electrode assembly (MEA), stability, conductivity, anion exchange ionomer, Platinum (Pt)-free catalyst
Full Abstract (Confidential)	This report presents a novel technique which was used to measure the conductivity, stability and performance properties obtained with the optimized anion exchange membrane (AEM) and anion exchange ionomer (AEI) developed during CREATE. The conductivity and stability of low-density polyethylene benzyltrimethylammonium LDPE-BTMA and FAA-3-5 AEMs were measured ex situ via a Scribner MTS 740. The AEI developed during CREATE was used in catalyst layers and combined with these membranes to further evaluate their in situ performance in anion exchange membrane fuel cells (AEMFCs) via a Scribner 850e fuel cell test station. With these initial results we show positive performance utilizing these novel materials and recommend that further testing be conducted to evaluate their long-term stability in AEMFCs.
Publishable Abstract (If different from above)	

REVISIONS			
Version	**Date**	**Changed by**	**Comments**
0.1	29.12.19	Dario R. Dekel	
	07.01.20	Rachel Backhouse	Added AEMEL data
	08.01.20	Frédéric Jaouen	Harmonization of AEI and AEM nomenclature

OPTIMIZED AEM & AEI: EX SITU CHARACTERIZATION AND TESTING IN AEMFC AND AEMEL

I. CONTENTS

II. INTRODUCTION

Anion-exchange membrane (AEM) degradation during fuel cell operation represents the main challenge that hampers the implementation of AEM fuel cells (AEMFCs). Reported degradation values of AEMs are difficult to reproduce since no standard methods are established. The present use of different techniques based on exposure of membranes to aqueous KOH solutions under different conditions and measuring different outputs during time, does not allow for a reliable and meaningful comparison of reported degradation data of different AEMs. We present a practical and reproducible ex-situ technique to measure AEM degradation in conditions that mimic *operando* fuel cell environment. In this novel technique, we measure the change of the true hydroxide conductivity of the AEM during time, while exposing it at different relative humidity conditions. The technique does not make use of liquid alkaline solution, simulating thus real fuel cell conditions and providing a good baseline for comparative degradation studies. We further investigated the performance of these membranes by integrating them into fuel cells made with ionomeric material obtained from FUMATECH to prepare the catalyst layers. Three different fuel cell tests were conducted; the first used benchmark Platinum (Pt)-based catalysts. In the second test we replaced the Pt-based anode with a novel Pt-free hydrogen oxidation reaction (HOR) catalyst. In the third test we present initial performance results utilizing the FAA-3-50 membrane. We also present results using the VM-FAA-3-50 membrane in AEM electrolyzer (AEMEL).

III. EXPERIMENTAL

Materials

AEM

- **LDPE membrane**: A highly conductive radiation-grafted anion-exchange membranes (RG-AEM) made from the peroxidation of (non-fluorinated) low-density polyethylene (LDPE).[1]
- **FAA-3-50:** A 50 µm-thick, highly conductive membrane from FUMATECH**.**
- **VM-FAA-3-50**: A 50 µm-thick, highly conductive membrane from FUMATECH**.**

AEI

- Fumion® FAA-3 ionomer: Anion-exchange material, polyaromate with quaternary ammonium group, a commercial product from FUMATECH
- Fumion® anion-exchange resin functionalized with TMA, developped during CREATE by FUMATECH
- **FC Anode Catalysts**
  1) PtRu/C catalyst (Alfa Aesar, 40% Pt and 20% Ru on carbon black, HiSPEC® 10000), henceforth labelled PtRu/C
  2) 10% Pd/CeO_2-C (nanoparticle Pd catalyst with a composite support made of Vulcan XC-72 carbon and CeO_2 (C-CeO_2))[2], henceforth labelled 10% Pd/CeO_2-C
- **FC Cathode Catalysts**
  1) Pt/C catalyst (Alfa Aesar, 40% Pt on carbon black, HiSPEC® 4000) henceforth labelled Pt/C
- **EL Anode Catalysts**
  1) Ni-foam/Ni_2P/$Fe(PO_3)_2$ (ICIQ)

EL Cathode Catalysts

1) Pt/C catalyst (ITM)
2) 10 wt% PtRu/SWNT-O_3 catalyst (Aalto)

AEM synthesis and characterization

- **AEM synthesis** - brominated poly(2,6-dimethyl-1,4-phenylene oxide) by three different bromination degrees (25,40 and 52%), was functionalized with TEA to obtain the PPO-TEA membranes.[3]
- **AEM characterization** – The membranes IEC was evaluated in Cl^- form by titration with $AgNO_3$ solution. Bicarbonate and true OH^- conductivities are measured using a 4-probe technique with a membrane test system (MTS 740, Scribner Associates Inc.) under a continuous 500 cm^3 min^{-1} N_2 (90% RH) environment.[4,5] The water uptake (WU) and WU kinetics of the AEMs were evaluated in their bicarbonate form, using VTI SA+ instrument (TA Instruments, USA) at 30ºC in water vapor at different humidity levels (45% and 90% RH).[6]

Fuel Cell MEA preparation and testing

The gas diffusion electrode (GDE) method was employed to prepare three 5 cm^2 anodes and cathodes for AEMFC testing.

Cell # 1

- Anode: PtRu/C was combined with fumion® AE resin and carbon black (Vulcan XC-72) to achieve an ionomer-to-catalyst ratio of 1:4.
- Cathode: Pt/C was combined with fumion® AE resin to achieve an ionomer-to-catalyst ratio of 1:4.
- Membrane: LDPE-BTMA

Cell # 2

- Anode: 10% $PdCeO_2$/C combined with fumion® AE resin to achieve an ionomer-to-catalyst ratio of 1:4.
- Cathode: Pt/C was combined with fumion® AE resin to achieve an ionomer-to-catalyst ratio of 1:4.
- Membrane: LDPE-BTMA

Cell # 3

- Anode: PtRu/C was combined with fumion® AE resin and carbon black (Vulcan XC-72) to achieve an ionomer-to-catalyst ratio of 1:4.
- Cathode: Pt/C was combined with fumion® AE resin to achieve an ionomer-to-catalyst ratio of 1:4.
- Membrane: FAA-3-50

Procedure

To make the inks for each electrode, the required amount of fumion® AE resin was combined with the catalyst, one-part of deionized water and two-parts of isopropanol, then ground with a mortar and pestle for 10 minutes to create a slurry. After sonication of the inks at 100% intensity for 1 h in a Grant XUBA3 ultrasonic bath filled with water and ice to keep the temperature below 5 °C, they were sprayed directly onto 5 cm^2 gas diffusion layers (Toray carbon paper, 060 - TGP-H-060 with 5 wt% PTFE wet-proofing) with an Iwata HP-TH professional airbrush. The anode and cathode catalyst loadings were 0.7 ± 0.15 $mg_{catalyst}$ cm^{-2}. AEMFCs were prepared in-situ with a 12.25 cm^2 piece of AEM sandwiched between the anode and cathode GDEs with Teflon gasketing giving a GDL compression of 25 – 35% and torqued to 4.5 Nm. The cells were tested in an 850e Scribner Associates Fuel Cell test station at various cell temperatures, with hydrogen and oxygen gases. The resultant polarization curves were measured at a scan rate of 10 mV s^{-1}.

Electrolyser MEA preparation and testing

$Ni_2P/Fe(PO_3)_2$ electrodes were prepared via a direct surface modification of the Ni support. The electrodes were functionalised with fumion® FAA-3 ionomer via spray deposition.
Pt/C catalyst was combined with fumion® FAA-3 ionomer in an ink and coated onto carbon paper support via spray deposition.
10 wt% PtRu/SWNT-O_3 catalyst was combined with fumion® AE resin in an ink and coated onto carbon paper support via spray deposition.
Fumapem® VM-FAA-3-50 membrane was ion-exchanged in 0.5 M NaOH with 3x solution changes.
AEMELs were tested in an ITM Power 8 cm^2 electrolyser cell with 0.1 M NaOH liquid electrolyte. Polarisation curves were measured under current control by stepping to each current and recording the voltage once steady state had been reached.

IV. Results and Discussion

Membranes

We used our recently developed ex situ method to measure the true OH^- conductivity in AEMs without the use of liquid electrolyte.[4] This method offers an opportunity to standardize conductivity measurements by determining the true OH^- conductivity simulating the real environment of an AEMFC during operation. In short, the method takes advantage of the reversibility character of the carbonation process[4,5,7,8] and exchange the (bi)carbonate anions by OH^- anions generated in situ by an external current. The applied current during the experiment causes the anions to move towards the anode, and the (bi)carbonates are released in the form of carbon dioxide.[4]

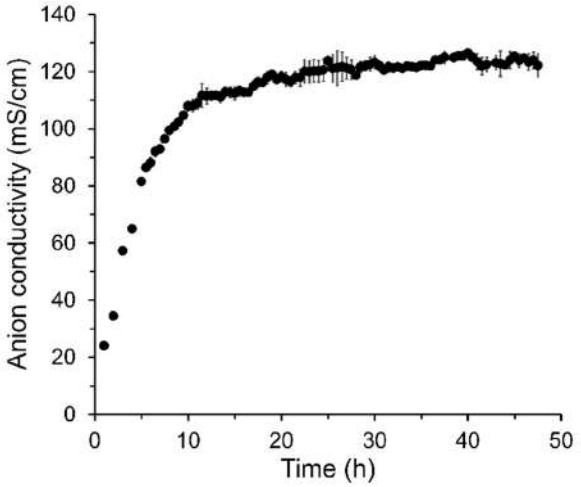

Figure 1. *Decarbonation process of an AEM using the ex-situ method of Ziv and Dekel[4], to measure the true OH^- conductivity of the membrane (55 µm thick low-density polyethylene radiation-grafted AEM functionalized with benzyl trimethyl ammonium (BTMA-LDPE) AEM[1,9,10]). The average and the standard deviations (shown by bars) of the conductivity are based on measurements of three different samples of the same AEM*

Using this method, we measured the anion conductivity during the decarbonation process of an LDPE-based radiation-grafted AEM as a function of time, until the plateau maximum value is reached (see Figure 1). This value is referred to the true OH^- conductivity of the membrane.[4] At the plateau, the AEM is in its full OH^- form, and we measure the drop in the value of true hydroxide conductivity as function of time. We use the technique to investigate the impacts of different and harsher environmental conditions on the AEMs and present a method to measure the degradation of AEMs in an environment that mimics an operating AEMFC. In the proposed technique, we measure the drop in the value of true OH^- conductivity as function of time at different (lower) relative humidity values.

The effect of relative humidity on the AEM stability

The resulting OH^- conductivity changes are then normalized to the initial conductivity values measured at different RH values, as shown in Figure 2.

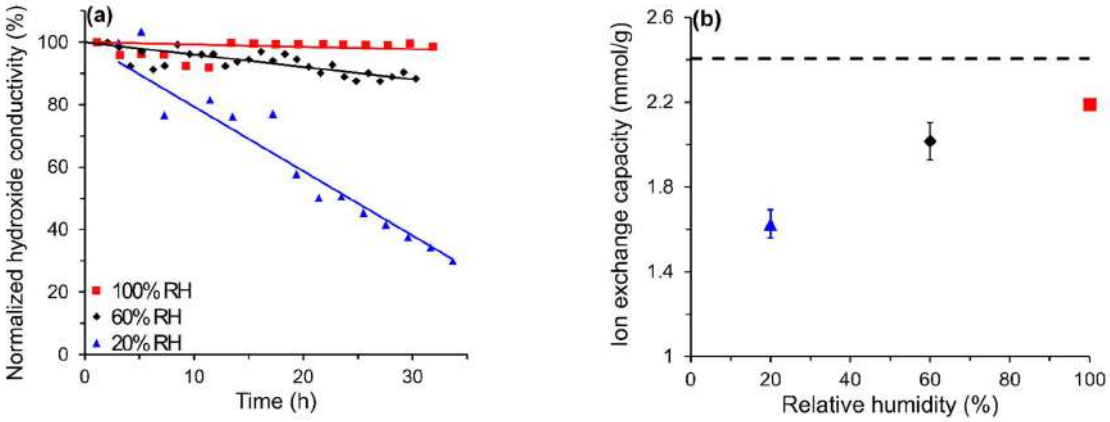

***Figure 2**. (a) The normalized true OH^- conductivity of the LDPE-BTMA AEM as a function of test time (80 °C, 100 µA and a nitrogen flow of 500 sccm/min) at different RH levels. (b) The final IEC of the AEMs measured after the degradation experiments shown in (a), as a function of the RH applied during the tests. The average and the standard error of the IEC are based on three measurements of the different samples of AEM. The dashed line marks the initial IEC of a fresh (non-degraded) membrane.*

The effect of temperature on the AEM stability

Figure 3 shows the change in normalized true OH^- conductivity at 65 °C, 80 °C, and 95 °C measured at 60 % RH, a representative humidity level at which the decrease in conductivity is largely noticeable. As expected, the degradation rate of the AEM increases with temperature.[11,12] While at 65 °C there is no evident degradation, at 80 °C and 95 °C the conductivity decay increases to 0.4 %/h and to 0.7 %/h, respectively. The IEC loss of the AEMs tested at different temperatures is shown in Figure 3b. The IEC dropped from 2.40 to 2.14 mmol/g at 65 °C, while it dropped to 2.02 and 0.49 mmol/g at 80 °C and 95 °C, respectively, confirming the increasing degradation caused by the increasing temperature of the proposed stability tests.

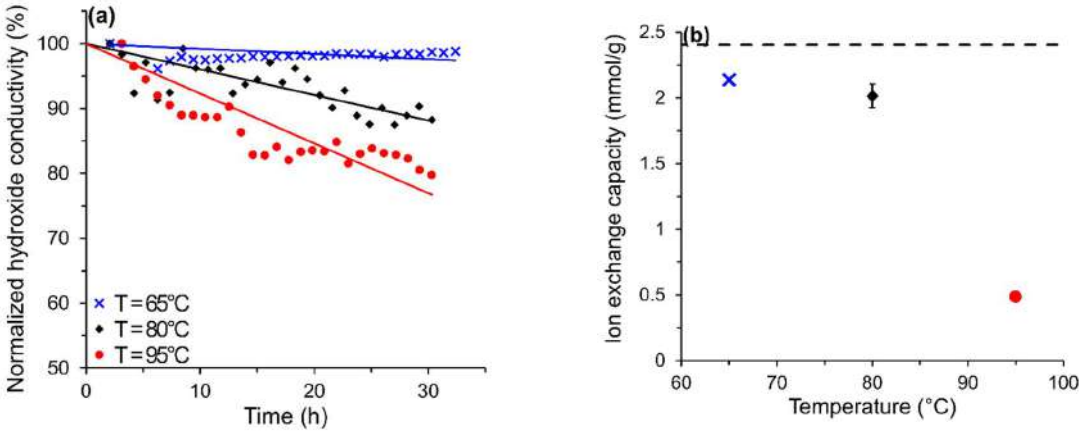

***Figure 3.** (a) The normalized true OH^- conductivity of the BTMA-LDPE AEM as a function of time (60 % RH, 100 µA and a nitrogen flow of 500 sccm/min) at different temperatures. (b) The final IEC of the AEMs measured after the degradation experiments shown in (a), as a function of the temperature applied during the tests. The average and the standard error*

of the IEC are based on three measurements of the different samples of AEM. The dashed line marks the initial IEC of a fresh (non-degraded) membrane

The change of AEM properties during degradation

The conversion time from bicarbonates to hydroxide was ca. 45 h for all membranes (Figure 4a). The bicarbonate and true OH^- conductivities[4] measured were 9.7, 3.2 and 1.8 mS cm^{-1}; and 43, 23, and 11 mS cm^{-1} for PPO-1.90, PPO-1.25, and PPO-1.19, respectively, in the range of previously reported PPO-based membranes.[13] The conductivity of the degraded AEMs was measured only for the HCO_3^-form. As expected, the IEC decreases during degradation time (Figure 4b), showing an exponential trend, typically exhibited in AEM studies.[14] After 30 days, PPO-1.25 and PPO-1.19 ion conductivities degraded almost entirely (>91%), while the conductivity of PPO-1.90 decreased by ca. 77%.

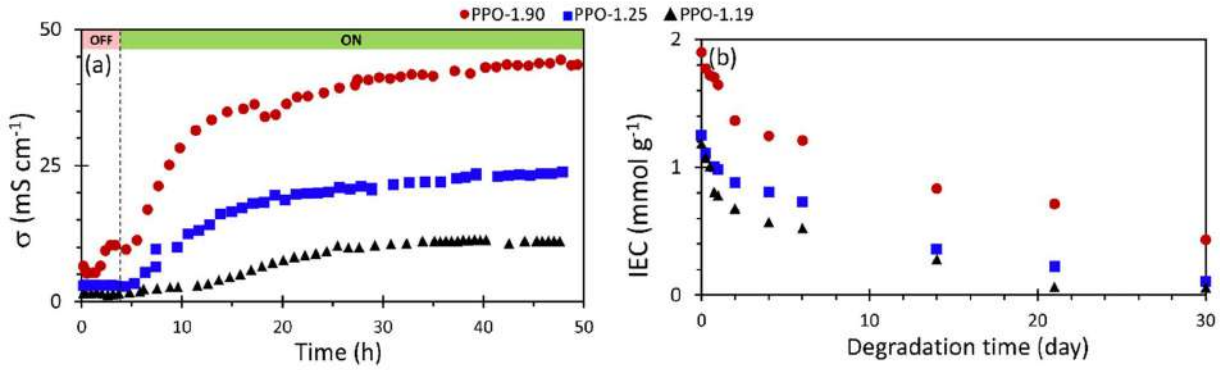

Figure 4. *(a) The HCO_3^- and true OH^- conductivities, measured at 30 °C and 90% RH. (b) AEMs' IEC values as a function of degradation time in 1M KOH 80°C.*

WU at different relative humidity (RH) were also measured during the degradation time (Figure 5). The initial WU values measured for PPO-1.90, PPO-1.25 and PPO-1.19 were 34%, 24% and 17% measured at high RH, and 12%, 9% and 7% measured at low RH, respectively. WU rapidly decreases within the first 14 days (ca. 300 h) of chemical degradation (Figure 5), but no significant loss in WU is exhibited after that. After 30 days, the WU of the PPO-1.90 decreases only ca. 39% at both RH levels. While at high RH PPO-1.25 and PPO-1.19 decrease by around 63%. At low RH, PPO-1.25 shows a less significant drop, losing 49% of its WU, while PPO-1.19 showed a 62% decrease. As expected, WU drops as a function of degradation time due to the decrease in IEC value. However, the decrease at high RH is more dominant than for low RH. As the membrane degrades, it can absorb less water from the atmosphere, however, for low RH it is relatively easier for the membrane to absorb water.[15]

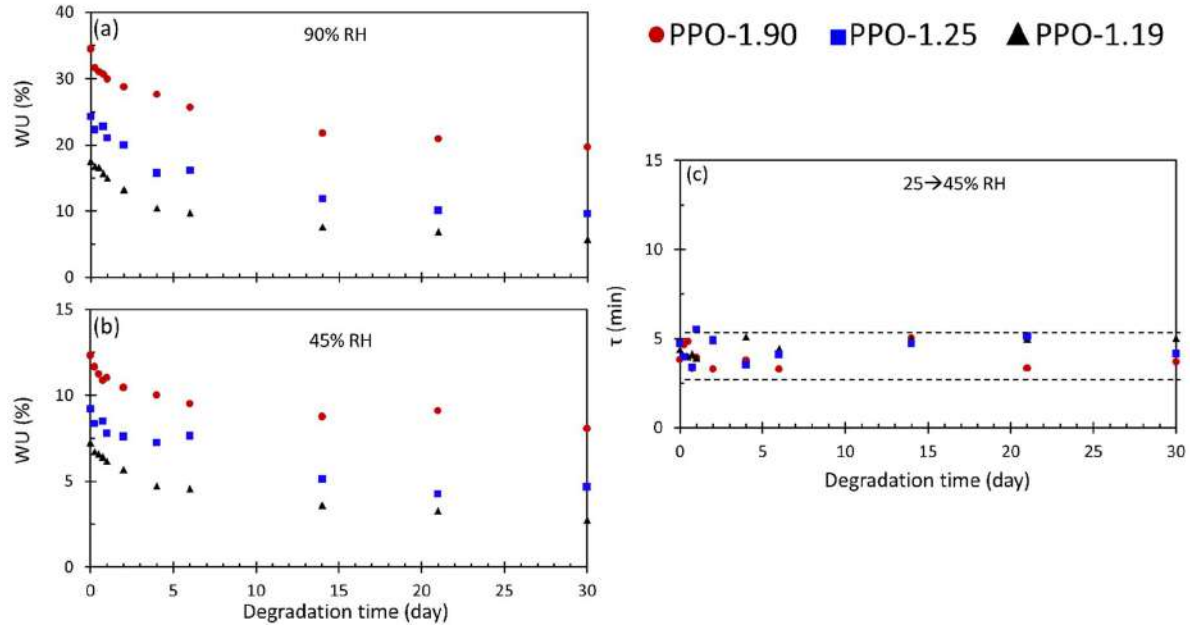

***Figure 5**. WU of the membranes (in their HCO_3^- form) as a function of degradation time in 1M KOH at 80℃. (a) WU measured at 90% RH, (b) WU measured at 45% RH, and (c) WU kinetics expressed by the characteristic time constant, ⍏, measured during a fast change in RH from 25% to 45%. Time constant τ was calculated by fitting the results to an exponential function, as described previously.[27]*

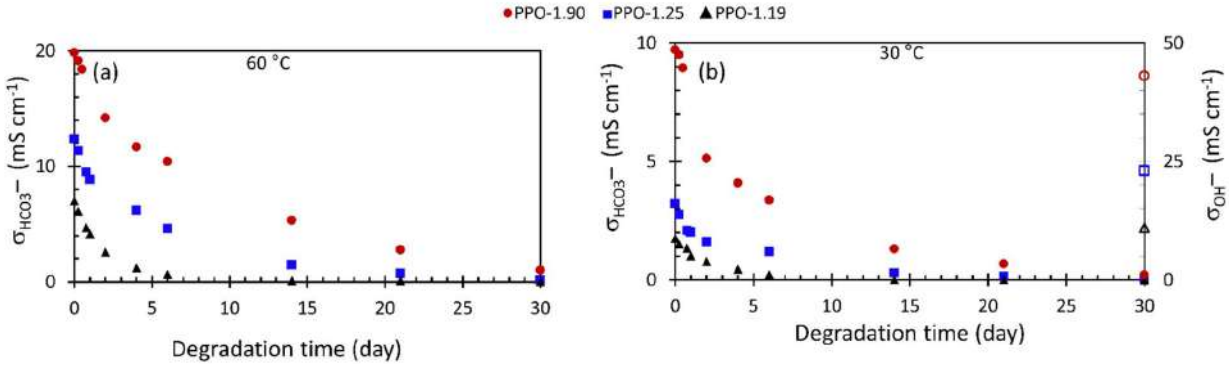

***Figure 6.** HCO_3^- conductivity as a function of degradation time measured at 90% RH and at (a) 60°C and (b) 30°C. Filled marks represent HCO_3^- conductivity; empty marks represent true OH^- conductivity data at the initial state of the AEMs before degradation (taken as the stabilized values in Figure 4a).*

AEM bicarbonate conductivity was measured as a function of the degradation time (Figure 6). As expected, PPO-1.90 demonstrates much higher initial conductivity, around threefold higher than that of PPO-1.19 and PPO-1.25 at 30 °C. Similar to the changes in IEC, there is a steady decline of conductivity throughout the degradation time. After 30 days, all membranes exhibit a larger decrease in conductivity as compared to their loss in IEC (see Figure 4b). For PPO-1.90, IEC declines by 77%, while the conductivity drops by 98% and 95% for 30 °C and 60 °C, respectively. For the case of the PPO-1.19, IEC drops to 95% and exhibit little to no anionic conducting properties (≥99% loss in conductivity at both 30 °C and 60 °C). PPO-1.25 shows similar results, a 91% decrease in IEC and ca. 98% decrease in conductivity. These results carried out at advanced chemical degradation stages enabled us to investigate membranes' properties in very low IEC ranges.

Using our ex-situ method, we measured the FAA-3-50 AEM at 40 and 60 °C at 95% RH, the results are presented Figure 7. The true hydroxide conductivity at 40 °C reached to 60 mS cm^{-1} and at 60 °C the conductivity passed the 100 mS cm^{-1} mark at a value of 115 mS cm^{-1}. The initial bicarbonate conductivity was 15. For further investigation the AEM was tested in-situ in an AEMFC.

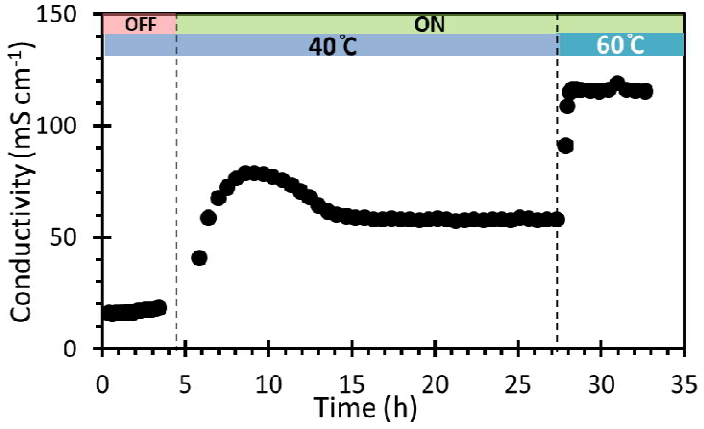

Figure 7. *Changes in the anion conductivity during the de-carbonation (CO_2 purging) process of FAA-3-50. The test was conducted at 0.1 mA direct current, N_2 flow, true OH^- conductivity was measured at 40 and 60 °C.*

AEMFCs

Figure 8 shows the results obtained with PtRu/C anode and a Pt/C cathode, loading of 0.7 ± 0.15 $mg_{catalyst}$ cm^{-2} per electrode with a LDPE-BTMA membrane. The anode and cathode were prepared as GDEs utilizing TMA functionalized Fuma ionomer. All testing was performed at 60 °C, with gas flow rates of 1 slpm at anode and cathode with no back pressurization. The fuel cell reached a peak power density (P_{max}) of over 1.6 W cm^{-2} and a limiting current density of over 3 A cm^{-2}. As can be seen from the polarization curves, minor changes to the anode and cathode dew points positively influenced the mass transport region without significantly impacting the peak power density, while extending the limiting current density. This indicates that additional optimization of the dew points of the gases, thereby balancing the water contained in the cell could improve the results even further.

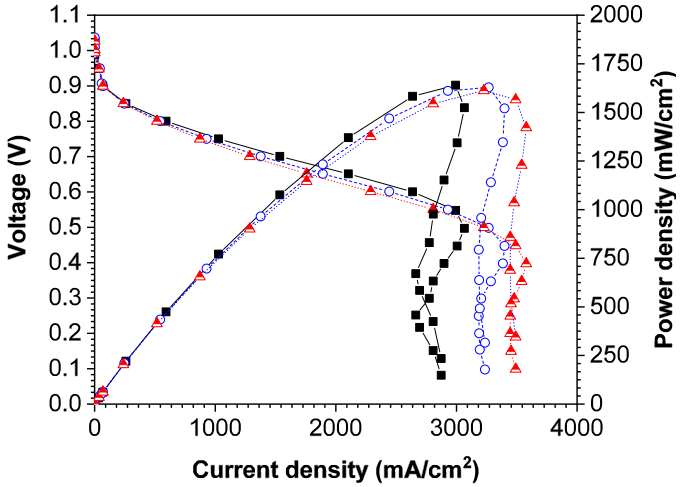

Figure 8*. Polarization and power density curves of a 5 cm^2 AEMFC with PtRu/C anode and Pt/C cathode, loading of 0.7 ± 0.15 $mg_{catalyst}$ cm^{-2} per electrode with a LDPE-BTMA membrane.* ■ *60 °C, hydrogen (1 slm, dew point 50.85 °C) and oxygen (1 slm, dew point 55.5 °C) gas flows with no back pressure.* ○ *60 °C, hydrogen (1 slm, dew point 50.8 °C) and oxygen (1 slm, dew point 52.9 °C) gas flows with no back pressure.* ▲ *60 °C, hydrogen (1 slm, dew point 49.9 °C) and oxygen (1 slm, dew point 52.4 °C) gas flows with no back pressure.*

Figure 9 shows the results obtained with Pd-CeO_2/C anode and a Pt/C cathode, loading of 0.7 ± 0.15 $mg_{catalyst}$ cm^{-2} per electrode with a LDPE-BTMA membrane. The anode and cathode were prepared as GDEs utilizing TMA functionalized Fuma ionomer. Testing was performed both at 60 °C and 70 °C, with gas flow rates of 1 slpm at anode and cathode. At 60 °C, the maximum performance was realized at optimized dew points in the anode and cathode with 2 barg of back pressure in the cathode. At 70 °C, the fuel cell reached a peak power density (P_{max}) of over 1.1 W cm^{-2} and a limiting current density close to 4.1 A cm^{-2} at full humidification at both electrodes and 1 barg back pressure at the cathode. These results show that high performance can still be attained by changing to a Pt-free anode. Furthermore, at the higher cell temperature, higher humidification is needed to balance the water in the cell to reach the maximum performance.

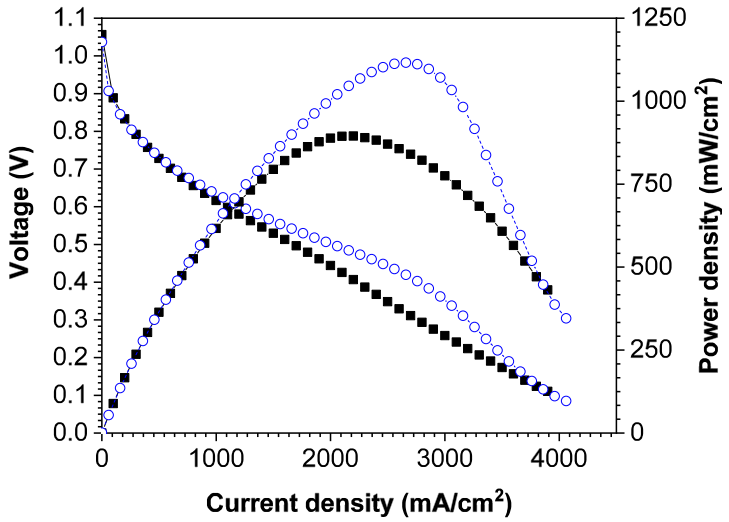

***Figure 9**. Polarization and power density curves of a 5 cm^2 AEMFC with Pd-CeO_2/C anode and Pt/C cathode, loading of 0.7 ± 0.15 $mg_{catalyst}$ cm^{-2} per electrode with a LDPE-BTMA membrane. ■ 60 °C, hydrogen (1 slm, dew point 50.9 °C) and oxygen (1 slm, 2 barg, dew point 53.6 °C) gas flows. ○ 70 °C, hydrogen (1 slm, dew point 70 °C) and oxygen (1 slm, 1 barg, dew point 70 °C) gas flows.*

Figure 10 shows the results obtained with PtRu/C anode and a Pt/C cathode, loading of 0.7 ± 0.15 $mg_{catalyst}$ cm^{-2} per electrode with a FAA-3-50 membrane. The anode and cathode were prepared as GDEs utilizing TMA functionalized Fuma ionomer. Testing was performed both at 60 °C with gas flow rates of 1 slpm at anode and cathode. The results compare the effect of full humidification at the electrodes to optimized humidification. The maximum performance was realized with optimized dew points in the electrodes and 1 barg of back pressure in the anode. This initially promising result with this very thin, highly conductive membrane indicates that further optimization of the dew points could lead to improved performance.

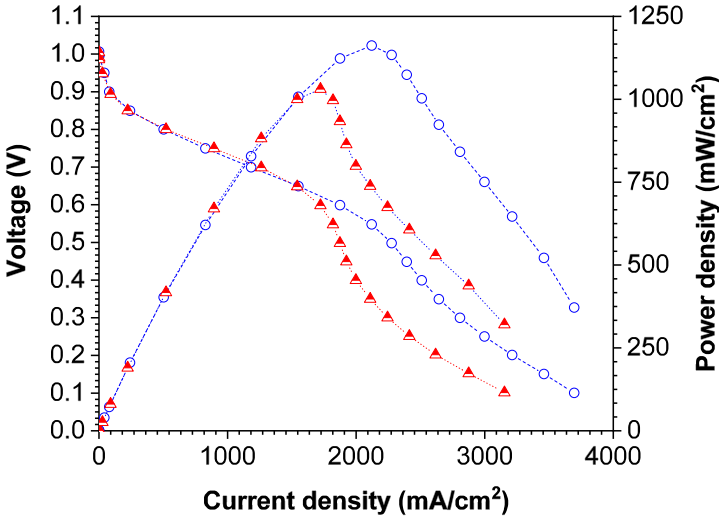

***Figure 10**. Polarization and power density curves of a 5 cm² AEMFC with PtRu/C anode and Pt/C cathode, loading of 0.7 ± 0.15 $mg_{catalyst}$ cm^{-2} per electrode with a FAA-3 membrane. ▲ 60 °C, hydrogen (1 slm, 1 barg, dew point 60 °C) and oxygen (1 slm, dew point 60 °C) gas flows. ○ 60 °C, hydrogen (1 slm, 1 barg, dew point 56 °C) and oxygen (1 slm, dew point 58 °C) gas flows.*

.

AEMELs

Figure 11 shows the results obtained with the fumapem® VM-FAA-3-50 membrane with 6.3 mg cm^{-2} ($Ni_2P/Fe(PO_3)_2$) at the anode and 0.23 mg cm^{-2} Pt at the cathode. The fumion® FAA-3 ionomer was used at both electrodes. Testing was performed at 45°C and 60°C.

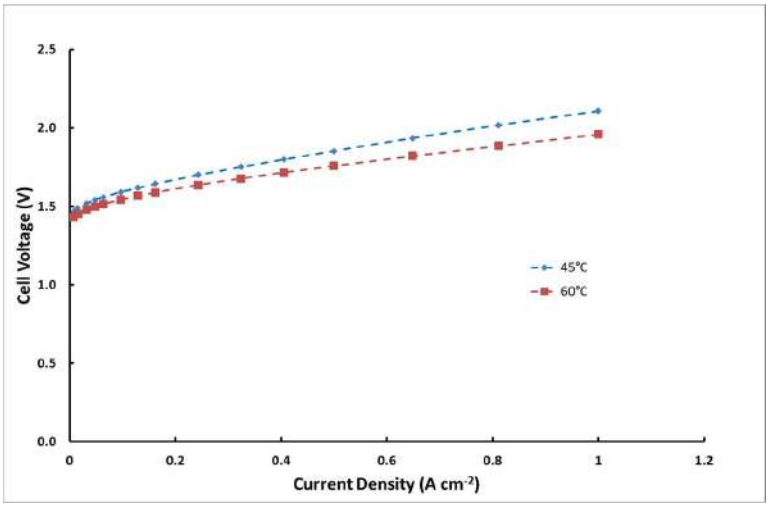

***Figure 11** Polarisation curves for an 8 cm² AEMEL cell with 6.3 mg cm^{-2} ($Ni_2P/Fe(PO_3)_2$) at the anode and 0.23 mg cm^{-2} Pt at the cathode and fumapem® VM-FAA-3-50 membrane at 45°C and 60°C.*

Figure 12 shows the results obtained with the fumapem® VM-FAA-3-50 membrane with 1.4 mg cm^{-2} ($Ni_2P/Fe(PO_3)_2$) at the anode and 0.01 mg cm^{-2} PtRu at the cathode. The fumion® AE resin was used at the cathode. Testing was performed at 45°C and 60°C. These results show that high performance can be achieved with an ultra-low CRM AEMEL.

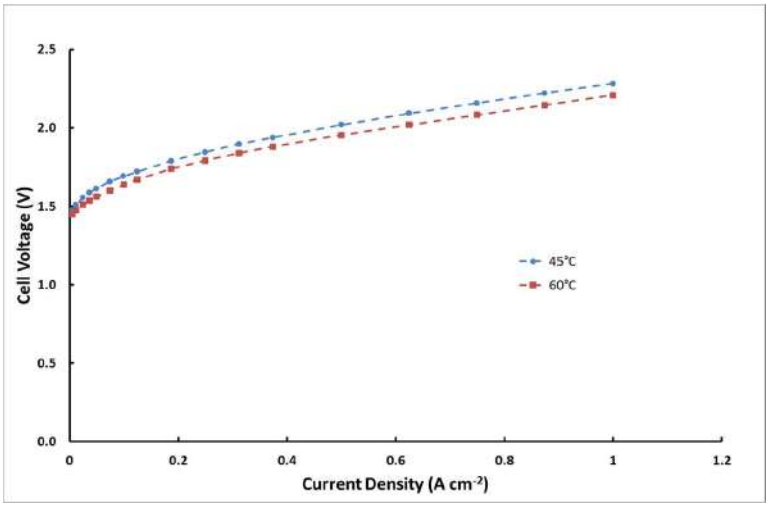

Figure 12 *Polarisation curves for an 8cm^2 AEMEL cell with 1.4 mg cm^{-2} ($Ni_2P/Fe(PO_3)_2$) at the anode and 0.01 mg cm^{-2} PtRu at the cathode and fumapem® VM-FAA-3-50 membrane at 45°C and 60°C.*

V. Conclusions

We present a practical, *ex situ* method for measuring the chemical stability of AEMs in a fuel cell-like environment. With this method, we conducted tests showing the degradation rate of a relatively stable AEM (LDPE-BTMA radiation-grafted AEM) at different RH values and different temperatures. We propose to use a sole parameter to characterize the membrane stability to be used for AEMFCs, we call the "AEM degradation parameter". For the LDPE-BTMA membrane, for example, this parameter was calculated to be 0.025 %/h/RH. In comparison with all current methods to measure chemical degradation of AEMs, this technique offers excellent reliability and reproducibility, as no liquid electrolyte (with all the involved complications) is used at any time of the test. This also assures to mimic the in-operando fuel cell environment, measuring then the real stability behaviour of an AEM during fuel cell operation.

We further tested LDPE-BTMA and FAA-3-50 membranes in 5 cm^2 AEMFCs using various catalysts in the electrodes made with the fumion® AE resin. The initial results are promising and show that we are capable of achieving very high performance with this new FUMA ionomer, comparable to that which is found in the literature.

AEMEL cells using the fumapem® VM-FAA-3-50 membrane, the fumion® FAA-3 ionomer and the fumion® AE resin with low-CRM cathode catalyst and CRM-free anode catalyst show promising performance.

VI. Recommendations and Future Work

- Measure the true hydroxide conductivity at higher temperatures.
- Study the ex-situ chemical stability of more AEMs.
- Evaluate polarization and longevity performance of PGM-free anode and cathode catalysts with the new fumion® AE resin, with optimized AEI to catalyst ratios.
- Evaluate performance and longevity of PGM-free anode and cathode catalysts with the FAA-3-50 membrane.

VII. REFERENCES

1. Wang, L.; Brink, J. J.; Liu, Y.; Herring, A. M.; Ponce-González, J.; Whelligan, D. K.; Varcoe, J. R. Energy Environ. Sci. 2017, 10 (10), 2154–2167.
2. Miller, H. A.; Lavacchi, A.; Vizza, F.; Marelli, M.; Di Benedetto, F.; D'Acapito, F.; Paska, Y.; Page, M.; Dekel, D. R. Angew. Chemie - Int. Ed. 2016, 55 (20), 6004–6007.
3. Willdorf-Cohen, S.; Mondal, A. N.; Dekel, D. R.; Diesendruck, C. E. J. Mater. Chem. A 2018, *6* (44), 22234–22239.
4. Ziv, N.; Dekel, D. R. Electrochem. commun. 2018, 88 (1), 109–113
5. Ziv, N.; Mondal, A. N.; Weissbach, T.; Holdcroft, S.; Dekel, D. R. J. Memb. Sci. 2019, 586, 140–150.
6. Zheng, Y.; Ash, U.; Pandey, R. P.; Ozioko, A. G.; Ponce-González, J.; Handl, M.; Weissbach, T.; Varcoe, J. R.; Holdcroft, S.; Liberatore, M. W.; Hiesgen, R.; Dekel, D. R. Macromolecules 2018, 51 (9), 3264–3278.
7. Ziv, N.; Mustain, W. E.; Dekel, D. R. ChemSusChem 2018, 11 (7), 1136–1150.
8. Krewer, U.; Weinzierl, C.; Ziv, N.; Dekel, D. R. Electrochim. Acta 2018, 263, 433–446.
9. Wang, L.; Peng, X.; Mustain, W. E.; Varcoe, J. R. Energy Environ. Sci. 2019, 1575–1579.
10. Wang, L.; Bellini, M.; Miller, H. A.; Varcoe, J. R. J. Mater. Chem. A 2018, 6 (31), 15404–15412.
11. Dekel, D. R.; Willdorf, S.; Ash, U.; Amar, M.; Pusara, S.; Dhara, S.; Srebnik, S.; Diesendruck, C. E. J. Power Sources 2018, 375, 351–360.
12. Marino, M. G.; Kreuer, K.-D. ChemSusChem 2015, 8 (3), 513–523.
13. Ge, Q.; Ran, J.; Miao, J.; Yang, Z.; Xu, T. ACS Appl. Mater. Interfaces 2015, 7 (51), 28545–28553.
14. Pan, J.; Han, J.; Zhu, L.; Hickner, M. A. Chem. Mater. 2017, 29 (12), 5321–5330.
15. Xu, K.; Hickner, M. A.; Ewing, C. S.; Wang, Q.; Mangiagli, P. M. Fuel Cells 2009, 9 (4), 432–438.